P10.11

HYDROMETEOR TYPE CLASSIFICATION IN WINTER CLOUDS USING X-BAND POLARIMETRIC RADAR MEASUREMENTS

- COMPARISON OF X-BAND POLARIMETRIC RADAR DATA WITH IN-SITU MEASUREMENTS BY HYVIS -

Koyuru Iwanami *[1], Kenichi Kusunoki [2], Narihiro Orikasa [2],
Masayuki Maki [1], Ryohei Misumi [1], and Masataka Murakami [2]
1: National Research Institute for Earth Science and Disaster Prevention (NIED), Tsukuba, Japan
2: Meteorological Research Institute, Tsukuba, Japan

1. INTRODUCTION

Hydrometeor type classification in precipitation clouds is useful for not only study of precipitation mechanisms but also disaster prevention by monitoring and/or forecast of hail and lightning, discrimination between rain and snow, and improvement of weather forecast through data assimilation. Polarimetric radar measurements of precipitation can be used effectively to classify hydrometeor types in precipitation because they are sensitive to the hydrometeor properties. Hydrometeor type classification using the fuzzy logic techniques has been proposed and there are two models of the product method (Liu and Chandrasekar 2000) and the additive method (Zrnić et al. 2001) in the interference stage of fuzzy logic classification system. Recently Lim et al. (2005) proposed a hybrid model that combined the additive method and the product method.

In order to develop hydrometeor classification method using X-band polarimetric radar measurements, simultaneous observations were carried out by the NIED X-band polarimetric radar (MP-X; Iwanami et al. 2001) and the hydrometeor videosondes (HYVIS; Murakami and Matsuo, 1990) in Niigata prefecture, Japan in December 2001. Characteristics of polarimetric measurements and temperature for five hydrometeor types were derived from comparisons of the MP-X and the HYVIS data. The beta membership functions in the fuzzification process of the fuzzy logic classification were specified based on the derived characteristics of polarimetric measurements for each hydrometeor type. Results of hydrometeor classification using fuzzy logic technique including a hybrid rule strength (Lim et al. 2005) and its verification are presented.

2. OBSERVATION AND DATA

2.1 *Observation*

Simultaneous observation was carried out by the NIED X-band polarimetric radar (MP-X; Iwanami et al. 2001) and the hydrometeor videosondes (HYVIS; Murakami and Matsuo, 1990) in Niigata prefecture, Japan for three weeks in December, 2001 by the National Research Institute for Earth Science and Disaster Prevention (NIED) and the Meteorological Research Institute (MRI). Observation area is shown in Fig. 1. MP-X radar site (R in Fig. 1) located on the southeastern slope of the Uonuma hills. Radar data were collected in the southeastern area of the site within 30 km range.

The balloons equipped with the hydrometeor videosonde (HYVIS) and a rawinsonde were launched at the surface meteorological observation site (M in Fig. 1) located 2.2 km southeast from the radar site.

Observations by the instrumented aircraft and millimeter-wavelength radar were also conducted because the other purpose of the field experiment was to investigate the feasibility of precipitation augmentation and cloud seeding from the aircraft.

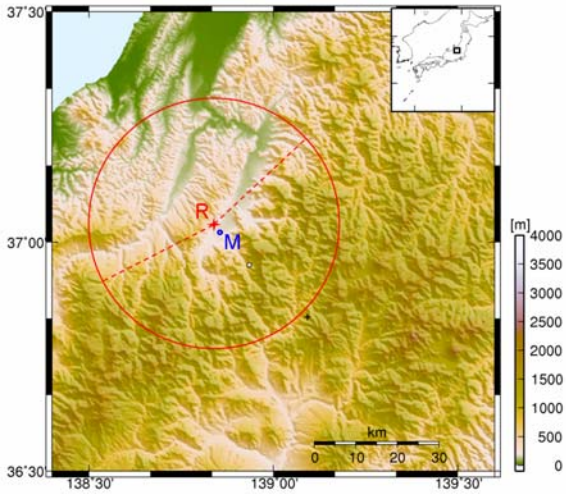

FIG. 1. Map of the observation area and the locations of MP-X radar site (R) and surface meteorological observation site (M). The red circle shows the MP-X radar observation range of 30 km.

2.2 *MP-X Radar*

Main specifications and a photograph of the NIED X-band polarimetric radar, MP-X (Iwanami et al. 2001), mounted on a 4-ton truck are listed in Table 1 and shown in Fig. 2, respectively. Radar data were collected by RHI scans during HYVIS observations considering their tracks. The range and angle resolutions and number of pulse integration was 100

* *Corresponding author address:* Koyuru Iwanami, National Research Institute for Earth Science and Disaster Prevention (NIED), Tsukuba 305-0006 Japan; e-mail: iwanami@bosai.go.jp

m, 0.5 degree and 256, respectively. The dwell time for one RHI scan was about 38 sec. The polar coordinate data by RHI scans were transformed to the Cartesian coordinate data with 500 m horizontal and 250 m vertical resolutions. Polarimetric measurements of reflectivity at horizontal polarization (Z_H), differential reflectivity (Z_{DR}) and correlation coefficient (ρ_{HV}) were mainly analyzed.

The MP-X radar has been removed from the 4-ton truck and set up on the top of the building in Kanagawa Prefecture, Japan in 2003, and used for rainfall observations in rainy season after that (Park et al. 2005).

TABLE 1. Specifications of the NIED MP-X radar.

Frequency	9.375 GHz
Beam Width	1.3 degree
Peak Power	50 kW
Pulse Width	0.5 μs
PRF	≤ 1,800 Hz
Polarization	SHV
Observation Range	≤ 80 km
Outputs	Z_H, V, W, Z_{DR}, ρ_{HV}, Φ_{DP}, K_{DP}

FIG. 2. A photograph of the NIED MP-X radar.

2.3 *HYVIS*

The hydrometeor videosonde (HYVIS) has been developed to measure the vertical distribution of hydrometeors in clouds by Murakami and Matsuo (1990). Two small TV cameras in the HYVIS take pictures of hydrometeors. The HYVIS and a rawinsonde are attached to the same balloon and launched into clouds, so that both particle images and meteorological data are collected simultaneously.

Fifteen balloons equipped with the HYVIS systems were launched during the field experiment and the data of nine HYVIS launches could be analyzed together with radar data. One-hour precipitation amounts and air temperature on the surface around their launch times were from 0 to 1.0 mm and from 0.1 to 6.9 °C, respectively.

The HYVIS data of the position, air temperature, and hydrometeor type were utilized in this analysis. Although hydrometeor types were at first classified into eight categories of water drop (R), sleet (S), graupel (G), aggregate (A), dendrite (D), column (C), plate (P), and needle (N) from the particle images, D, C, P, and N were classified into one category of single ice crystal (X) in the following analysis.

3. CHARACTERISTICS OF POLARIMETRIC MEASUREMENTS FOR HYDROMETEOR TYPES

Characteristics of polarimetric measurements of reflectivity at horizontal polarization (Z_H), differential reflectivity (Z_{DR}) and correlation coefficient (ρ_{HV}) and temperature (T) for five hydrometeor types, that is, water drop (R), sleet (S), graupel (G), aggregate (A) and ice crystal (X), were derived from comparisons of MP-X and HYVIS data.

The position of HYVIS was compared with the plane of RHI scan, then the sets of radar and HYVIS data were picked up on conditions that the time difference was less than 3 minutes and the horizontal distance between the position of the HYVIS and the plane of RHI scan was less than 1.5 km.

Table 2 shows the number of HYVIS image data for each hydrometeor type picked up for comparisons between polarimetric measurements and hydrometeor types on the conditions described above. There were a few hydrometeor types in one HYVIS image in many cases. In such cases, those different hydrometeor types were compared with the same polarimetric parameters in one mesh on RHI data, that is, the numbers in the column ‘Multi’ in Table 2 include overlap. If another condition that there was only one type of hydrometeor in one HYVIS image was added, the numbers of HYVIS image data decreased by 4 (A) to 54 % (R) shown in the column ‘Single’ in Table 2.

TABLE 2. The number of HYVIS image data for each hydrometeor type. See text.

Hydrometeor Type	Number of HYVIS Image Data	
	Multi	Single
R: Water Drop	485	262
S: Sleet	188	67
G: Graupel	973	198
A: Aggregate	326	12
X: Ice Crystal	2179	589
Total	4151	1128

Frequency that each polarimetric parameter and air temperature has some value was derived from comparing picked-up radar and HYVIS data for each hydrometeor type. The results using the sets of data including overlap described above are shown in Fig. 3.

4. HYDROMETEOR TYPE CLASSIFICATION

For hydrometeor type classification, fuzzy logic technique including a hybrid model proposed by Lim et al. (2005), which combined the additive method and the product method in the interference stage, was used. The beta membership functions, that are important for classification performance,

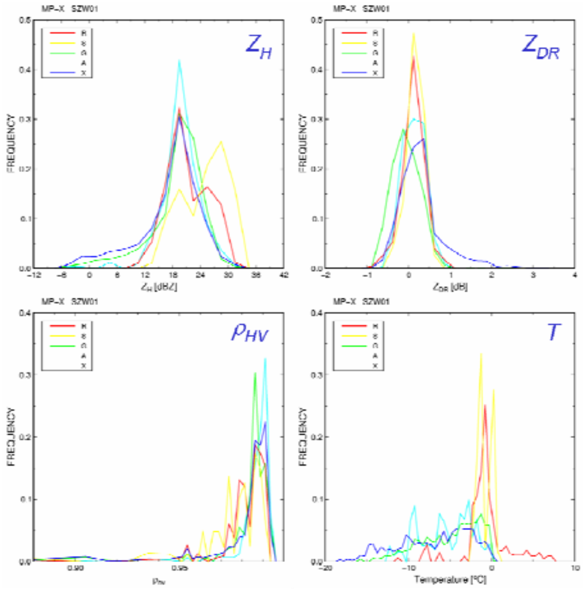

FIG. 3. Frequency polygons of polarimetric parameters of Z_H, Z_{DR} and ρ_{HV}, and air temperature (T) for the hydrometeor types of R (red line), S (yellow line), G (green line), A (light blue line), and X (navy blue line).

were specified based on the derived characteristics of polarimetric measurements for each hydrometeor type described in section 3.

Figure 4 shows an example of the results of the hydrometeor type classification with the RHI images of polarimetric measurements of Z_H, Z_{DR}, and ρ_{HV} at 07:35:46 LST December 16, 2001. Each width of the beta membership function was set to the range of 70 % of accumulated frequency of polarimetric measurements and temperature from the maximum(s) to both sides.

The hydrometeor types detected by HYVIS and classified by the method were compared for validation. The rates of 'hits' to 'false alarm' for type R, S, G, A, and X were 62, 68, 60, 23, and 28 %, respectively. The reasons why it was more difficult to identify correctly aggregate (A) and ice crystal (X) were considered that aggregate (A) was detected together with the other types of hydrometeor in almost all HYVIS images, and ice crystal (X) include originally four kinds of hydrometeors with different characteristics of particles then with wide range of polarimetric measurements in snow clouds.

5. SUMMARY AND ISSUES

X-band polarimetric radar data were collected simultaneously as *in-situ* measurements with hydrometeor videosonde (HYVIS) in winter clouds. Both data were compared and frequency polygons of polarimetric measurements and temperature for hydrometeor types were derived. Results of hydrometeor classification using fuzzy logic technique

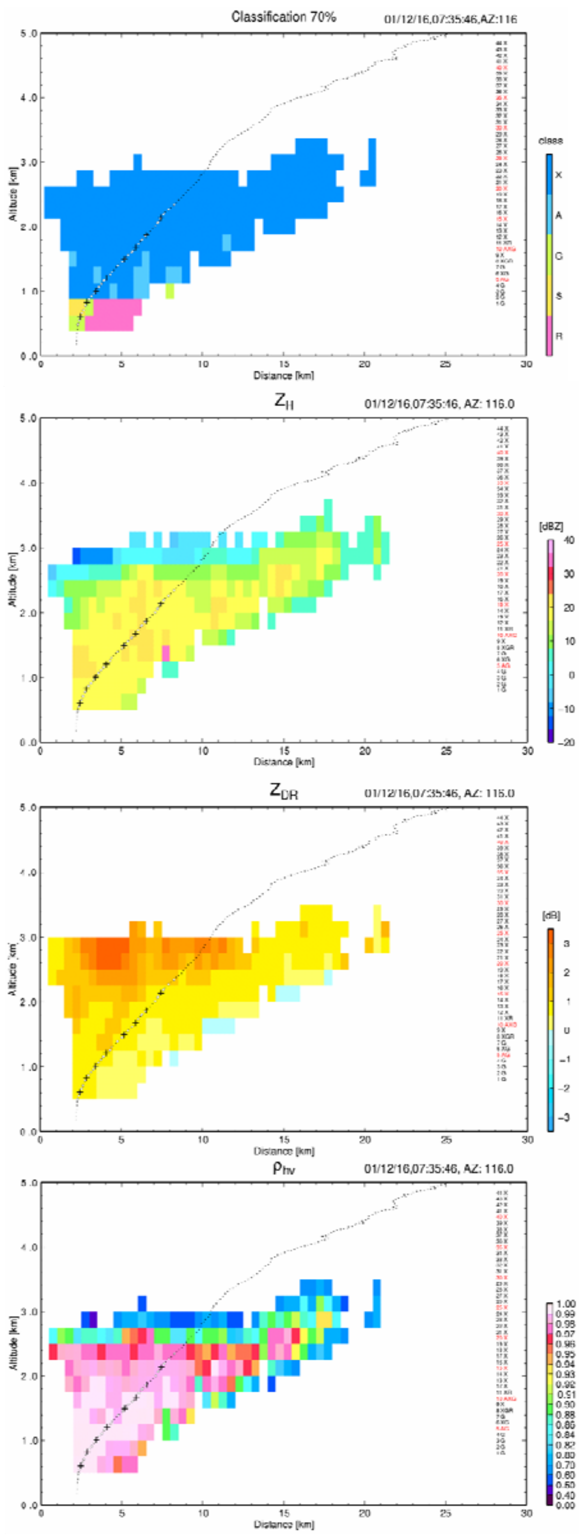

FIG. 4. Hydrometeor classification result and RHI images of Z_H, Z_{DR}, and ρ_{HV} at 07:35:46 JST on Dec. 16, 2001. Dotted line, marks of open circle and cross show the HYVIS track and the positions of HYVIS image data, respectively.

including a hybrid rule strength (Lim et al. 2005) and its verification were also reported. The beta membership functions were specified based on the derived characteristics of polarimetric measurements and temperature for each hydrometeor type.

Another polarimetric measurement of specific differential phase (K_{DP}) will be added as an input parameter after the improvement of the filtering method of differential propagation phase (Φ_{DP}) to estimate K_{DP}. In-situ observation data by the Instrumented aircraft can be utilized for validation of the classification method.

NIED plans to construct X-band polarimetric radar network in metropolitan area in Japan and carry out observations from 2008 rainy season. To extend the application of the method to summer precipitation clouds, characteristics of polarimetric measurements for rain, melting layer and hail are expected to be incorporated by using the MP-X radar data collected in summer season from 2001 to 2006.

ACKNOWLEDGEMENTS. The authors would like to acknowledge Dr. S.-G. Park for supporting radar observation. One of the authors (KI) thanks Mr. Kento Tanimura and Mr. Ippo Suzuki from Tsukuba University, Japan for their effort of programming.

REFERENCES

Iwanami, K., R. Misumi, M. Maki, T. Wakayama, K. Hata, and S. Watanabe, 2001: Development of a multiparameter radar system on mobile platform. *Proc. 30th Intern'l Conf. Radar Meteor.,* 104-106.

Lim, S., V. Chandrasekar, and V. N. Bringi, 2005: Hydrometeor classification system using dual-polarization radar measurements: Model improvements and in situ verification. *IEEE Trans. Geosci. Remote Sensing*, **43**, 792-801.

Liu, H., and V. Chandrasekar, 2000: Classification of hydrometeors based on polarimetric radar measurements: Development of fuzzy logic and neuron-fuzzy systems, and in situ verification. *J. Atmos. Oceanic Technol.*, **17**, 140-164.

Murakami, M., and T. Matsuo, 1990: Development of hydrometeor videosonde. *J. Atmos. Oceanic Technol.*, **7**, 613-620.

Park, S.-G., M. Maki, K. Iwanami, V. N. Bringi, and V. Chandrasekar, 2005: Correction of radar reflectivity and differential reflectivity for rain attenuation at X band. Part II: Evaluation and application. *J. Atmos. Oceanic Technol.*, **22**, 1633-1655.

Zrnić, D. S., A. Ryzhkov, J. Straka, Y. Liu, and J. Vivekanandan, 2001: Testing a procedure for automatic classification of hydrometeor types. *J. Atmos. Oceanic Technol.*, **18**, 892-913.